Low energy charged particles interacting with amorphous solid water layers

Yonatan Horowitz and Micha Asscher

Citation: J. Chem. Phys. **136**, 134701 (2012); doi: 10.1063/1.3697870
View online: http://dx.doi.org/10.1063/1.3697870
View Table of Contents: http://jcp.aip.org/resource/1/JCPSA6/v136/i13
Published by the American Institute of Physics.

Low energy charged particles interacting with amorphous solid water layers

Yonatan Horowitz and Micha Asscher
Institute of Chemistry, The Hebrew University of Jerusalem, Edmund J. Safra Campus, Givat-Ram, Jerusalem 91904, Israel

(Received 28 December 2011; accepted 23 February 2012; published online 2 April 2012)

The interaction of charged particles with condensed water films has been studied extensively in recent years due to its importance in biological systems, ecology as well as interstellar processes. We have studied low energy electrons (3–25 eV) and positive argon ions (55 eV) charging effects on amorphous solid water (ASW) and ice films, 120–1080 ML thick, deposited on ruthenium single crystal under ultrahigh vacuum conditions. Charging the ASW films by both electrons and positive argon ions has been measured using a Kelvin probe for contact potential difference (CPD) detection and found to obey plate capacitor physics. The incoming electrons kinetic energy has defined the maximum measurable CPD values by retarding further impinging electrons. L-defects (shallow traps) are suggested to be populated by the penetrating electrons and stabilize them. Low energy electron transmission measurements (currents of 0.4–1.5 μA) have shown that the maximal and stable CPD values were obtained only after a relatively slow change has been completed within the ASW structure. Once the film has been stabilized, the spontaneous discharge was measured over a period of several hours at 103 $\pm$ 2 K. Finally, UV laser photo-emission study of the charged films has suggested that the negative charges tend to reside primarily at the ASW-vacuum interface, in good agreement with the known behavior of charged water clusters. © *2012 American Institute of Physics*. [http://dx.doi.org/10.1063/1.3697870]

I. INTRODUCTION

Low energy electrons interacting with their surrounding liquid and solid materials are among the most fundamental, abundant, and important chemical events. Electron transfer reactions at the solid-liquid interface constitute the basic step in electrochemistry but can be found in photo-catalysis and biologically important phenomena such as photosynthesis and radiation medicine. Many reviews were written over the years on the polarizing effect of electrons on liquid media that lead to their stabilization, once the solvent molecules rearrange and reorient to minimize the free energy of the system.[1,2] At this stage the electrons are considered solvated. The interaction of electrons with bulk liquid water is certainly the best studied and most important.[3] In contrast to their reasonably well understood interactions with homogeneous media, the chemistry and physics of electrons at the solid/liquid and, in particular, at the solid/vacuum interface has been less investigated, therefore, not as well understood.[4]

The dynamics of electron solvation has been studied in recent years by injecting electrons from a metallic or oxide substrates into overlayer of condensed molecules by employing fs pulsed laser sources. Using two photon photoemission methods, the subsequent reorientation of the solvent molecules, leading to the final solvation could be probed in real time.[4–6] A complimentary family of experiments where electrons transmission through a molecular film has revealed the wavelength dependence (spectroscopy) and adlayer structure effects on electrons transmission.[7–10] Other processes where low energy electrons colliding with a molecular film lead to ions and neutral fragments ejection back to the vacuum have also been investigated as a result of reactive electron attachment phenomena.[11–13]

Many of the above studies have focused on condensed water films in the form of amorphous solid water (ASW), prepared at substrate temperature below 145 K, or on crystalline ice films, obtained by preparing the film above 150 K.[14]

These studies were in most cases limited to only a few layers of condensed molecules, otherwise electrons could not be injected into and transmitted through the film.

Electron stimulated desorption (ESD) of charged and neutral products at the low energy range were reported.[13,15] Specifically, at the energy range 0–20 eV, D^- is the dominant ionic product following ESD of a D_2O film with a peak at 7.2 eV, while the minor products are O^- and OD^-.[16] All these were formed via direct or indirect dissociative electron attachment mechanism.[7]

The interaction of electrons with thicker layers of adsorbed molecules, of the order of few hundred monolayers (ML), has very rarely been addressed.[12,17–19] The effect of strong electric fields on the physical and chemical properties of ASW has been investigated, showing that for ASW films, grown at a temperature range of 105–150 K, field ionization of water molecules occurs at electric fields above 0.2 V/Å.[18] Moreover, the magnitude of the field directly affects the phase transition temperature (ASW to CI), decreasing by 20 K down to 130 K.[18]

"Bjerrum defects"[17,20] which are intrinsic hydrogen dislocations, usually marked as: L for two adjacent oxygen atoms (a hydrogen vacancy) and D for two adjacent hydrogen atoms. These L/D defects are considered as the main charge carriers

in ASW and crystalline ice. Ionic defects (OH^- and H_3O^+) are considered as the minor charge carriers.

In this study we focus our attention at this intermediate solid water film thickness of 120–1080 ML. We have investigated simultaneously low energy (1–25 eV) electrons transmission (current measurements) and charging (contact potential difference – CPD measurements) as a function of film thickness. We found that charging is stable for hours below 120 K and that steady state transmission currents are electron energy, time, and film thickness dependent.

II. EXPERIMENTAL

The experiments described here were conducted in a previously described[21] ultrahigh vacuum (UHV) system at a base pressure of $\sim 2 \times 10^{-10}$ Torr. A 0.6×0.6 cm^2 Ru(0001) single crystal is daily cleaned via a 10 min sputter using high energy ions (Ar^+ at 700 eV) with subsequent flash annealing to 1620 K and then stay at 1400 K for two more minutes. The sample was cooled by a liquid nitrogen Dewar down to 100 K and further cooled to 90 K upon pumping on top of the filled LN_2 reservoir. C type thermo-couple wires (W26%Re/W5%Re) were spot welded on the back side of the sample providing input for the sample temperature control algorithm at accuracy of ±1 K. Connecting a low noise bias voltage (18 V battery) to the Kelvin probe (KP – Besocke Delta Phi) electronics enables measuring CPD values in the range of ±30 V. Combining the CPD measurements and mass spectrometry (RGA 300 – SRS) to the temperature programmed desorption (TPD) routine enabled us to follow the work function changes (ΔΦ-TPD) that the ASW undergoes as a function of temperature (structural deformations) prior to any water desorption during standard ΔP-TPD mode. Triple distilled water (were further purified by three "freeze-pump-thaw" cycles), and all other gasses are introduced via a precision leak valve by back filling the UHV chamber. The final exposure is calculated in Langmuir (L) units (1 L $= 10^{-6}$ Torr × s) where 1.5 L equals 1 ML, derived from the onset of ice multilayer desorption peak near 160 K. The Ar^+ ions used for ASW positive charging were generated by a standard ion sputter gun (Varian). The ion's kinetic energy used in this study was fixed at ≈55 eV ± 5 eV, their flux measured as electrical current between sample and ground was typical at $\approx 10^{-8}$ A range. An electron gun (ELG2 – Kimball physics) has generated a constant current of -1.5×10^{-6} A as measured on a clean Ru(0001) sample at 110 K. This current has been maintained over the different electron energies (3–25 eV) we employed in these measurements. A 6 min exposure time to electrons for negative charging studies was constant for all energies. Auger electron spectrometer (LK Technology) enabled control over the surface elemental composition before and following exposure and charging of the ASW layer. Photoemission measurements of the negatively charged films were performed using UV photons generated by an excimer laser (MPB Technologies Inc. – PSX-100). The laser provides 2.5 ns long pulses at 248 and 193 nm of about 1 mJ/pulse, and variable repetition rate up to 100 Hz. The UV photons pass through a special fused silica window onto the UHV chamber.

III. RESULTS AND DISCUSSION

A. Positive charging

ASW films exposed to positive low energy ion beam (LEIB) result in a negative change of the CPD measured by the KP due to accumulation of positive charges within the film. As was previously demonstrated, CPD obtained following exposure to positive (H_3O^+) LEIB reveals a linear CPD dependence on the films thickness.[22]

These results are consistent with a classic parallel plate capacitor, presented in Eq. (1),

$$\Delta V = \frac{Qd}{A\varepsilon_{(T)}\varepsilon_0}, \tag{1}$$

where a linear dependence between the measured voltage and layer thickness is expected. ΔV [volts] is substituted by the measured CPD and corresponds to the voltage that develops across the ASW film. Q is the total charge [coulomb], d [meters] is the distance between the plates (or film thickness where 1 ML $= 3.96 \times 10^{-10}$ m),[23] A [m^2] is the surface area of the "plates" (sample dimensions), while ε_0 and $\varepsilon_{(T)}$ are the vacuum permittivity and the temperature dependent dielectric constant, respectively, $\varepsilon_{(T)} = 3.2$ (Refs. 12, 13, and 25) at 100 K. Based on Eq. (1), a CPD drop of 0.02 V per monolayer was derived (see Fig. 1). An important question arises is it possible for 55 eV Ar^+ ions to be embedded within the ASW matrix. As expected, TPD measurements at mass 40 of Ar following the positive charging by Ar^+ ions have ruled out this possibility at the surface temperature (100 K) of our experiments. The first ionization energy of Ar atoms[24] is 15.75 eV and the ionization threshold for ice is 11.0 eV.[25] Therefore, the following mechanism: $Ar^+ + (H_2O)_n \rightarrow Ar + (H_2O)_n^+$ is energetically favorable by almost 5 eV. Another possible mechanism, known from low energy (1–10 eV) proton – solid water collisions,[26] is

$$Ar^+ + 2H_2O_{(ad)} \rightarrow H_3O^+ + ArOH$$
$$\rightarrow Ar + OH + H_3O^+_{(ad)}.$$

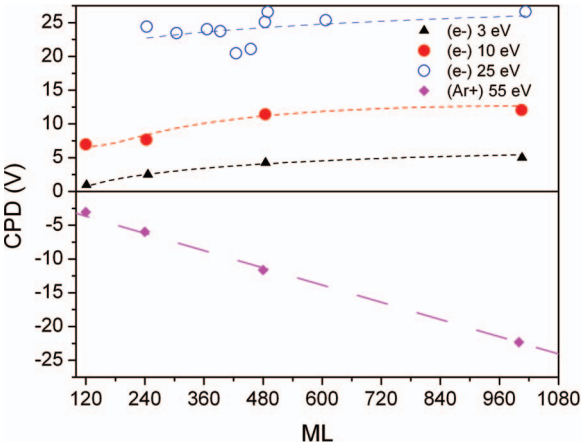

FIG. 1. Upper section: CPD (V) values as a function of ASW film thickness (ML) and incident electron kinetic energies (3–25 eV) are presented. Lower section: CPD evolution as a function of ASW film thickness (ML) after Ar^+ low energy ion beam (LEIB) at constant kinetic energy (≈55 eV). All ASW films were initially annealed to 120 K, cooled to 100 K and subsequently exposed to either ion or electron irradiation for 6 min.

A similar mechanism was suggested for fluorine positive ion – ASW collision:[27] $F^+ + (H_2O)_n \rightarrow F + (H_2O)_n^+$ ($\Delta E = -4.8$ eV), proposed to explain the observed inhibition of the ESD of F^+ ions from preadsorbed PF_3 layers when capped by ice. Efficient charge transfer and neutralization of the Ar^+ ions combined with the slow mobility of protons at surface temperature lower than 150 K can explain the accumulation of positive charges and consequently the capacitor-like behavior of ASW films that were subjected to LEIB. Moreover, it was further demonstrated that instead of migrating to a metallic substrate, H_3O^+ ions formed within ASW film prefer to accumulate at the ice-vacuum interface.[17]

In Fig. 1, CPD values obtained following 6 min exposure to Ar^+ ions (55 eV) or electrons at various kinetic energies are displayed as a function of ASW film thickness. Indeed the linear behavior of the ASW charging as a result of the Ar^+ ions bombardment could be explained reasonably well using Eq. (1) for a parallel plate capacitor, apparently originates from the ionization of few monolayers at the ASW film-vacuum interface. If these ions are immobile at 100 K, then the main attributing variable to the CPD should be the distance between this charged layer and the substrate.

In order to further examine our claim above we have followed the stability of the charged ASW films in time, maintaining the surface temperature at 100 ± 5 K. In Fig. 2, the CPD decay is demonstrated for 100–240 ML ASW films. As can be seen the main drop of CPD occurs within the first 10 min by almost 30% of the initial value and to about 50% after an hour, the maximum duration of these measurements.

A simple capacitor discharge model: $V_{(t)} = V_0 e^{-\frac{t}{RC}}$, fits well the data, where $V_{(t)}$ and $V_{(0)}$ are the contact potential difference values measured (in volts) after time t and at the initial point ($t = 0$), respectively. In our experimental setup, termination of Ar^+ bombardment cycle and the onset of CPD measurements has been separated by a fixed time gap of 90 s. Here, t is the time measured in seconds, R is the resistance, and C is the capacitance of the ASW film. The fitted exponential decays were found to be in good agreement with the recorded data as can be seen in Fig. 2. The V_0 values used for the best fit in Fig. 2 were −3.5, −5.3, −7.0, −8.0 V for the 100 ML, 140 ML, 200 ML, and 240 ML, respectively. The difference in the V_0 values reflects faster initial decay of the thinner layers. However, trying to evaluate the *RC* coefficients in terms of physical resistance or capacitance from the fit has proven inconclusive at this point, requiring further investigation.

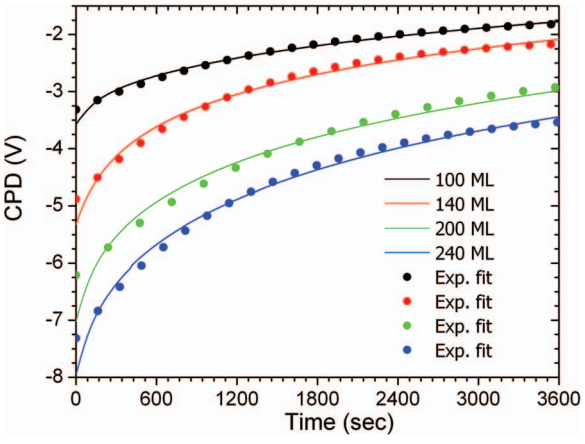

FIG. 2. Solid curve: CPD (V) decay over an hour of 100–240 ML thick ASW films after 6 min exposure to Ar^+ LEIB at 55 eV. Dots: an exponential fit according to a plate capacitor discharge formula: $V_{(t)} = V_0 e^{-\frac{t}{RC}}$. The averaged RC coefficient is 1400 ± 250 s, regardless of film thickness.

B. Negative charging

1. Charge accumulation

Bombardment of ASW layers by low energy electrons results in an asymptotic behavior of the measured CPD. The maximal CPD voltage is dictated by the incoming electrons kinetic energy. A similar effect was reported in the case of oxygen molecules acting as electron traps on top of a Kr multilayer[7] that performed as the dielectric bulk. In our case the electrons are stabilized at local potential traps induced by the (incomplete) hydrogen bond matrix.[28] Consistent with the basic concepts of low-energy electron transmission[29] spectroscopy, a retarding field develops by the accumulation of electrons within the samples' bulk[28] or on its surface.[30] Hence, the maximum CPD value measured as a result of a given energy was strongly correlated with the incident electrons' kinetic energy (3–25 eV) rather than with the ASW film thickness. Verification procedure of the electrons charging and retardation effects is described below and summarized in Fig. 3.

The sample was exposed first to 5 eV electrons for 6 min, followed by a 10 min period of CPD measurement in which the measured CPD has decayed to its anticipated value as expected after a 10 min discharge time. Similar results were obtained for initial runs at higher electron energies (up to 25 eV). Subsequent exposures of the already charged film by electrons at energy higher by 5 eV have enabled the electrons to overcome the retarding field of the previous run and as a result the CPD had increased by 5 V. Figure 3 "staircase" plot reflects this effect. The ASW film was not annealed between

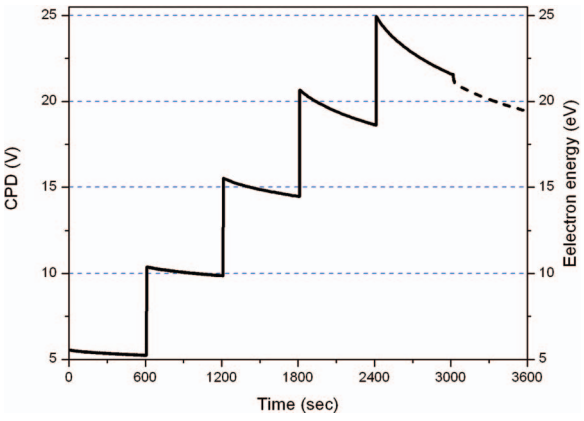

FIG. 3. The measured CPD (V) and its spontaneous decay for a 480 ML thick ASW film. The same film was exposed to consecutive periods of 6 min electron irradiation at increasing e^- - beam energy intervals of 5 eV. The natural decay of the charge was recorded for the subsequent 10 min. Note the dashed curve (starting at ≈ 3000 s) where 20 eV electrons exposure hits when the films' CPD is higher than 20 V. This exposure resulted in no further accumulation of charge, i.e., the CPD continues to decay, unaffected.

successive electron exposures in order to preserve the solvated electrons. Exposure of any of the charged films to electrons at lower energy results in no change in the measured CPD except for the anticipated degree of discharge. This observation is shown for the 25 eV electrons in Fig. 3. This film was subsequently bombarded by 20 eV electrons (dashed curve at the end of the 25 V "stair" in the upper right part of Fig. 3). No CPD increase demonstrates and verifies the retarding nature of the charged film with respect to lower energy electrons.

Following electron bombardment of ASW film, a positive CPD has been measured (negative charging). No linear correlation was found to the film thickness, as in the case of the positive charging. The retarding field that gradually forms limits the measured CPD to the incident electrons kinetic energy, as discussed above.

The simplified view presented here for both negative and positive charging and their complex interactions with ASW films can be justified under two limiting assumptions: (a) the dielectric constant of frozen water ($\varepsilon_{(T)}$) is practically temperature independent at the temperature range of the experiments, namely, 90–160 K. For the case of H_2O and D_2O crystalline ice films at thicknesses ranging from a few hundreds to several thousands layers at temperatures below 120 K, it was demonstrated that the dielectric constant is indeed temperature independent, at a value of $\varepsilon_{(T)} = 3.2$.[12,13,25] By monitoring the $CPD_{(T)}$ while sampling the surface temperature we observed that the onset for a dielectric discharge is around 110 $\pm$ 2 K for films grown at 90 K. This onset temperature is in good agreement with the literature data[15] demonstrating that the maximal dipole reorientation, as a result of pre-annealing is obtained at 120 K. Performing charging experiments by always having a pre-annealing step at 120 K ensures a stable and identical state of ASW film before exposure to the e^--beam.

The second assumption is that the thickness of the ASW film will always be significantly smaller than the root square of the charged area.[17] This assumption does not require any specific charge distribution within the bulk of the charged film, yet a parallel plate capacitor is expected to form under these conditions. At film thickness of 1000 ML (~400 nm) or thinner with an e^--beam spot size that covers the entire sample area (0.4 cm^2), the above assumption is always valid. The plate capacitor behavior requires that the charge will primarily reside at the ASW – vacuum interface. This will be verified below by performing laser induced charge depletion measurements. Although the validity of a plate capacitor is not straightforward when negative charge is concerned it becomes more apparent when one plots the accumulated charge vs. ASW layer thickness. In Fig. 4, the accumulated charge is presented as a function of film thickness. The charge of each layer was calculated using Eq. (1) above, while the voltage (V) and layer thickness (d) were experimentally determined.

The dashed curve in Fig. 4 is the theoretical charge as calculated for an ideal parallel plate capacitor with a fixed 25 V CPD and a dielectric constant $\varepsilon_{(T)} = 3.2$. The red dots reflect the amount of charge *derived* from Eq. (1) based on experimental CPD values obtained shortly after (<30 s.) 360 s exposure of the film to 25 eV electrons. The accumulated charges vs. the number of multilayer follows a 1/d (d = film thickness = distance between plates) behavior, as indeed is expected from a plate capacitor.

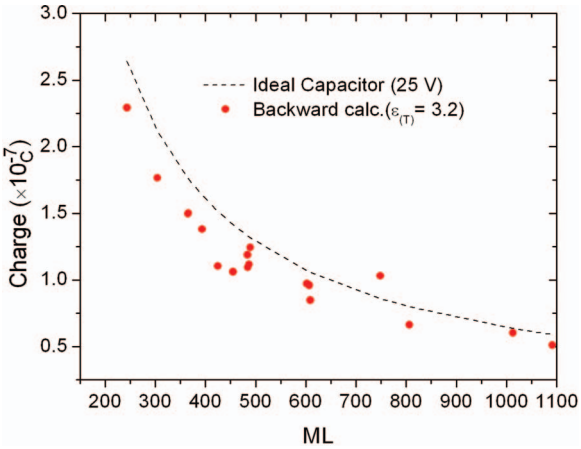

FIG. 4. Dashed curve: The theoretical charge (Q) accumulation in an ideal parallel plate capacitor (see Eq. (1)) as a function of ASW thickness with a steady CPD of 25 V and $\varepsilon(T) = 3.2$. Dots: The calculated charge according to experimental CPD values and ASW film thickness, while the temperature was kept constant at 100 K, at this temperature $\varepsilon(T) \approx 3.2$.

Based on previous experiments, the stability of L-defects in ice films is known to be kept to about 110 K.[31–33] Such L-defects are often considered as shallow electron traps, energetically residing below the electronic conduction band of ice. This kind of traps is likely to be populated by the impinging electrons and stabilize them. Moreover, the sharp drop of the CPD values at any ASW film thickness upon annealing to 110 K and to 130 K for crystalline ice films, strongly supports the hypothesis that these structural defects are responsible for the charge accumulation and stabilization.[34]

2. Charging stability

The main observable arising from examination of the charging levels depicted in Fig. 3 is the following: As the kinetic energy of the incoming electrons increases the capacitor discharges faster. The $CPD_{(t)}$ decay in time, presented in Fig. 5, clearly demonstrates this observation. This

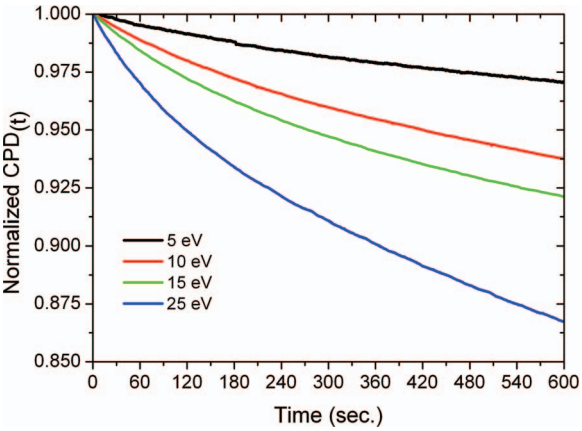

FIG. 5. Normalized $CPD_{(t)}$ (V) decay (limited to the first 10 min) of a 480 ML thick ASW films following 6 min exposure to the indicated incident electron kinetic energies. The time between termination of the charging step and onset of CPD (V) measurements was fixed to 100 s.

phenomenon can be explained by the electric fields' magnitude inside the bulk that operates on the solvated electrons. The incoming energetic electrons lose all memory (their initial momentum and kinetic energy[9]) upon solvation, becoming just point charges that are stabilized by the water molecules surrounding them. Since the thickness of the ASW film in Fig. 5 was fixed at 480 ML and the temperature maintained well below 110 K, we can assume that the dielectric properties of the film were constant and identical at the different electron exposures. Therefore, the only change is the electric field magnitude that has developed in accordance with the incoming electrons energy (5–25 eV). The lower the applied field is the slower the electrons will migrate to the substrate. The similarity of the decay plots at energies 10 and 15 eV (see Fig. 5) might originate from 10.4 to 14.5 eV. Frenkel[35] excitons reported to be located at this energy range in the conduction band of the ASW. [36]

Since these are dissociative excitons, once electron-hole pair is formed the kinetics should be on the same time scale for the two kinetic energies as can be seen in Figs. 3 and 5. For 5 and 25 eV there are available electronic bands associated with the anti-bonding $2a_1$ and $4a_1$ bands;[36] thus, the solvated electrons are more strongly affected by the field strength. Yet another possibility is that 25 eV electrons are more energetic than the threshold energy for ionization of ASW,[27,28] suggesting that the charge transport mechanism through the bulk in pure ASW and ice can also originate from Bjerrum (L and D are hydrogen displacements) and ionic defects that develop in the hydrogen bonded matrix.[37–39] The activation barrier for formation and separation of D and L hydrogen dislocations (D – for two facing hydrogen atoms, L – for the two atoms directed away from each other) are about 0.7 eV and 1.0 eV, respectively, in the case of ionic (H_3O^+, OH^-) defects.[40] For pre-existing L-defects, which are generated as the water monolayers adsorb, and in the presence of an electric field the activation barrier is even lower.[39] Therefore, a gradually stronger electric field that is generated by the accumulated charges (25 V corresponds to $\approx 1.3 \times 10^6$ V/cm) will undoubtedly produce a higher repulsive potential for such defects. This accumulated field eventually forces solvated negative charges towards the grounded metallic substrate.

C. Electrons transmission

The absolute value of the electrical current transmitted through ASW layers and its time dependence were found to be sensitive to the ASW thickness as shown in Fig. 6 for 25 eV electrons. The variation of the measured current with time includes initial decay that varies between a few seconds at the thickest ASW samples, up to 20 min in the case of the 360 ML sample. The initial current decrease reflects the gradual saturation of as prepared, low coordination sites,[40–42] effectively increasing bulk ASW resistivity.

The high bulk density of intrinsic L – defects known to exist in ASW grown at ~100 K may explain the gradually shorter time needed to accumulate the same number of electrons at the thicker films, determined by the final, stable CPD value of the respected films, of 24 ± 1 V. In contrast, in crystalline ice, the intrinsic low coordination sites are scarce.

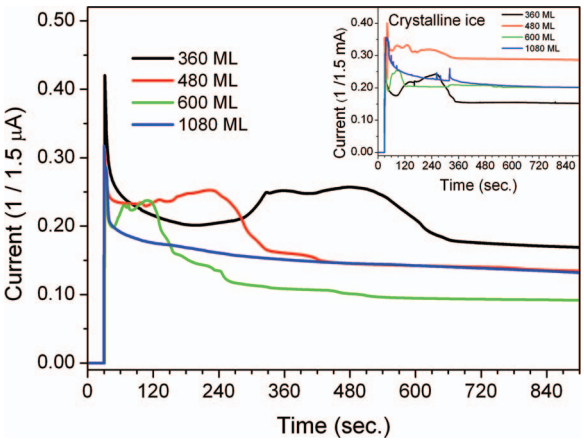

FIG. 6. Relative values, normalized to the current measured on the clean ruthenium surface (1.5 μA), of the electrical currents transmitted through ASW layers (360–1080 ML) and their time dependence while exposed to 25 eV electrons. Inset: Relative current transmission vs. time measurements through crystalline ice films at the indicated ice thicknesses.

Therefore, the main charge carriers are L – defects that are created by the incoming electrons due to their growing field effect as they accumulate. Hence, the steady state between incoming electrons and transmitted ones is achieved faster. In addition the crystalline nature of the bulk allows for better transport routes of charge carriers through well-developed conduction bands. This manifests itself in the higher (about twice) steady state transmission currents measured through CI films compared to ASW, see Fig. 6 inset. After the initial decay, a peak in the current evolves, back to about 25% of the initial current measured on the clean metal followed by a second decay to the final, stable steady state current value. The maximal and stable CPD value (at different electron energies) was obtained only after the relatively slow change in ASW structure has been completed, leading to the peak current formation. In other words, within the period of time in which the current goes through a maximum the solvation process of electrons within the ASW film has been associated with internal structural modifications that have affected the degree of electrons transmission through the ASW film in a slow, dynamic way.

We will address separately the rise and fall of the current peak following the initial decay: (a) *Increase*: The increase in the conductivity after some time of accumulated charges that has led to the initial current drop, (film thickness dependent) may be attributed to the fact that L-defects are now *generated* as a byproduct of dangling H-bonds that reorient in order to accumulate and stabilize the excess electrons.[29,32,43] Since the water molecules point their hydrogen ends towards the solvated electron, six L type vacancies are now facing outwards.[44] Under the influence of the electric field that has developed, these vacancies move via zigzag hydrogen reconfigurations down to the substrate.[32] (b) *Decrease*: The second drop of the current after reaching a local maximum can be explained assuming that every traverse route of L-defects in the bulk forms a barrier for a new L-defect (or OH^- ion), thus increasing the effective film's resistivity that leads to a decrease in the measured current. Moreover, after some time the threshold charge required to establish a retarding field has

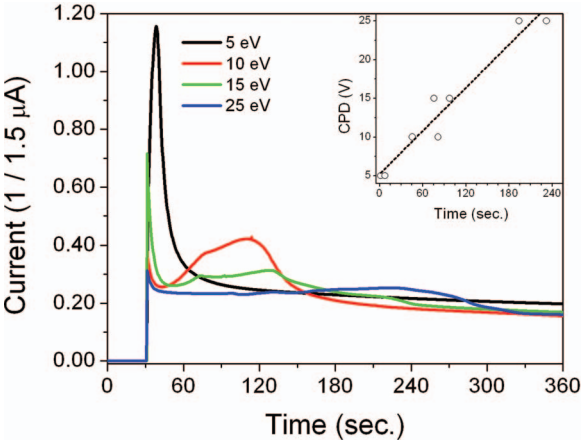

FIG. 7. Normalized currents transmitted through 480 ML ASW films and their time dependence while exposed to 5–25 eV electrons. Inset: Peak-current position in time (s) vs. CPD (V).

been acquired; therefore, most of the incoming electrons will now be repelled away from the surface. A steady state between incoming and outgoing current has been established. The absolute steady state outgoing current in this stage, reflecting transmitted electrons through the ASW film, is somewhat sensitive to the ASW film thickness (Fig. 6) and temperature (not shown). Another aspect regarding the nature of the solvation process is revealed by examining the time it takes to reach maximal charge capacity of the ASW film. In Fig. 7, normalized current versus time is plotted for various incoming electron energies. The accumulation time needed to reach the current – peak is shortest for 5 eV electrons and the longest for 25 eV electrons, while the 10 and 15 eV are in intermediate time duration.

Rearranging Eq. (1) to $Q = C \times \Delta V$, where C represents the constants: $C = \frac{A\varepsilon_{(T)}\varepsilon_0}{d}$, suggests that the amount of charge (Q) required to reach the retarding voltage (ΔV) displays a linear proportion. In our study the kinetic energy of the incident electrons and the maximal voltage (CPD) are identical. Hence, for a lower voltage, fewer charges are needed to be accumulated at a fixed initial current. In other words less exposure time is needed at lower energies. In addition, the mean free path of electrons in solids decreases as their energy increases from 5 eV to 25 eV by approximately a factor of 5;[45] therefore, the low energy electrons will be transmitted against a smaller effective resistance, arising from fewer electron scattering events. A linear plot of CPD (V) vs. time is shown as an insert in Fig. 7.

We conclude that the increased electric field at a fixed charging level, by increasing the distance between capacitor plates (the ASW film thickness) is the main driving force for the shorter time required to reach steady state CPD in thicker films (600–1080 ML) compared to the thinner ones (360, 480 ML), see Fig. 6.

D. Photo-emission of solvated electrons

Several studies addressing the interaction of electrons with water nanoclusters have shown that excess electrons tend to reside on the ice-vacuum interface of clusters.[5,6,46] However, the location of electrons on macro flat surfaces is yet to be determined. In order to find where the solvated electrons prefer to reside in our system, the following measurements were preformed: A 480 ML thick film, charged by 25 eV electrons was irradiated by 248 nm (5 eV) photons, originated from a KrF excimer laser. Electrons were photo-emitted, resulting in gradual neutralization of the charged ASW film, as indicated by nulling the CPD signal. In addition, similarly charged films were capped with fresh monolayers of water ranging from 96 to 480 ML. The capping process has practically not affected the results of photoemission or the measured CPD value. The number of photoemitted electrons was calculated by subtracting the mean $CPD_{(t)}$ after 10 min of natural decay (this value was obtained from former experiments, e.g., Fig. 5) from the $CPD_{(h\nu)}$ measured right after laser irradiation. The number of photo-emitted electrons is thus obtained by rearranging Eq. (1): $\Delta Q = C \times \Delta CPD$, and dividing the photo-emitted charges (ΔQ) by the charge of an electron. The apparent cross section for photo-induced neutralization or photo-emitted electrons has been extracted from a first order exponential fit to the decay of measured CPD vs. number of UV photons. The results are displayed in Fig. 8.

By applying a first order exponential decay, we obtained a neutralization/photoemission cross section of $\sigma \approx 1.4 \pm 0.5 \times 10^{-19}$ cm^2 regardless of the presence and thickness of the capping layer. No direct ionization of ASW is expected[47–50] at 248 nm, and indeed no evidence for ejected electrons and/or water molecules or their derivatives were detected from a neutral, uncharged 480 ML ASW film (data not shown) after prolong exposures to 5 eV photons. We, therefore, conclude that for the 25 eV charged film the above cross section is the value for photo-induced ionization and ejection of solvated electrons from the ASW film.

CPD decay from its initial value near 25 V as a result of photon irradiation, $CPD_{(h\nu)}$, is shown in Fig. 9. For comparison the spontaneous natural drop of $CPD_{(t)}$ at the same period of time is also shown (open circles) after 6 min. The $CPD_{(h\nu)}$ values in Fig. 9 were obtained after subtracting the relevant spontaneous drop in $CPD_{(t)}$ measured after 6 min, the time of exposure to electrons and laser irradiation.

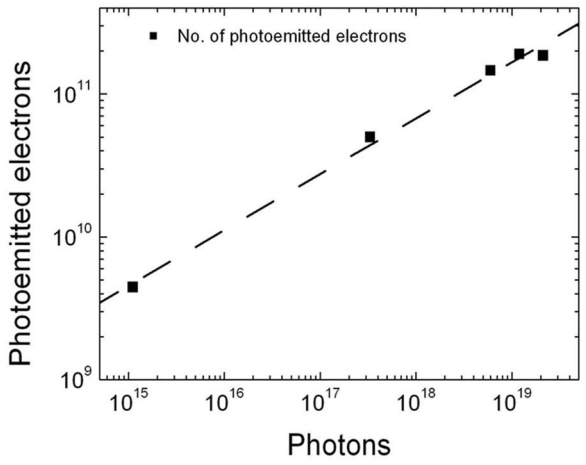

FIG. 8. KrF Excimer laser (5.0 eV) photo-emitted electrons from ASW – vacuum interface vs. the number of photons. The dashed line is a guide to the eye.

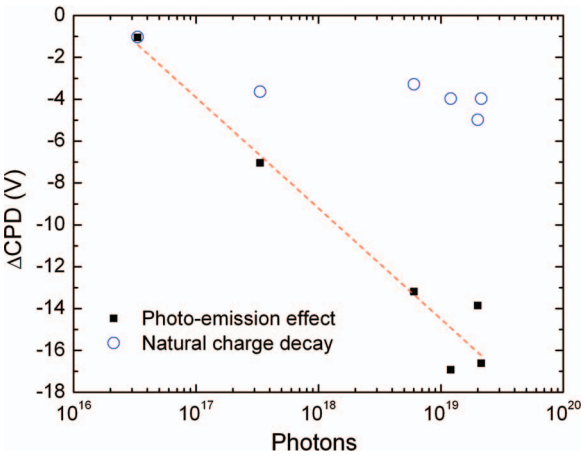

FIG. 9. (■) CPD drop from an initial value of 25 V due to photo-emitted electrons is plotted vs. the number of photons. (○) The spontaneous drop in CPD after 10 min.

Considering the mean free path values of relevant low energy electrons, we conclude that the electrons tend to accumulate near the ASW – vacuum interface regardless of the capping film thickness and the initial electrons kinetic energy. This is rather similar to the behavior of electrons interacting with water clusters[51] and of protons.[17]

IV. CONCLUSIONS

The interaction of ASW films with low energy electrons and positive argon ions has developed into a plate capacitor-like behavior. Collisions of positively charged argon ions (at 55 eV) result in a linear decrease in the measured CPD value as the ASW layer becomes thicker. In the case of electrons, an increase of the CPD to a maximum value has been dictated by the incoming electrons energy in the range (3–25 eV) due to retardation of the further impinging electrons. Monitoring the transmitted electrons through the films has revealed that only after a slow (minutes time-scale) reorientation of hydrogen bonds in the solid water matrix, manifested as an increase in the total current the maximal and stable CPD has been obtained. The hour long natural discharge at temperatures below the activation temperature (110 K) for hydrogen bond defects diffusion has led us to suggest that the accumulation of the negative charges is carried out primarily by intrinsic L-defects that act as shallow traps residing just beneath the ASW conduction band. We conclude that the solvated electrons are preferentially residing near the ASW-vacuum interface, as indicated from UV laser photoemission measurements.

[1]M. A. Henderson, Surf. Sci. Rep. **46**(1–8), 5–308 (2002).
[2]C. R. Arumainayagam, H.-L. Lee, R. B. Nelson, D. R. Haines, and R. P. Gunawardane, Surf. Sci. Rep. **65**(1), 1–44 (2010).
[3]E. J. Hart and M. Anbar, *The Hydrated Electron* (Wiley-Interscience, New York, 1970).
[4]J. Zhao, B. Li, K. Onda, M. Feng, and H. Petek, Chem. Rev. **106**(10), 4402–4427 (2006).
[5]J. Staehler, U. Bovensiepen, M. Meyer, and M. Wolf, Chem. Soc. Rev. **37**(10), 2180–2190 (2008).
[6]U. Bovensiepen, C. Gahl, J. Stahler, and M. Wolf, Surf. Sci. **584**(1), 90–97 (2005).
[7]R. M. Marsolais, M. Deschenes, and L. Sanche, Rev. Sci. Instrum. **60**(8), 2724–2732 (1989).
[8]S. K. Jo and J. M. White, J. Chem. Phy. **94**(8), 5761–5764 (1991).
[9]R. Naaman and L. Sanche, Chem. Rev. **107**(5), 1553–1579 (2007).
[10]G. Perluzzo, G. Bader, L. G. Caron, and L. Sanche, Phys. Rev. Lett. **55**(5), 545–548 (1985).
[11]N. G. Petrik and G. A. Kimmel, J. Phys. Chem. C **113**(11), 4451–4460 (2009).
[12]X. N. Pan, H. Abdoul-Carime, P. Cloutier, A. D. Bass, and U. Sanche, Radiat. Phys. Chem. **72**(2-3), 193–199 (2005).
[13]J. Herring-Captain, G. A. Grieves, A. Alexandrov, M. T. Sieger, H. Chen, and T. M. Orlando, Phys. Rev. B **72**(3), 035431 (2005).
[14]Y. Lilach, M. J. Iedema, and J. P. Cowin, Surf. Sci. **602**(17), 2886–2893 (2008).
[15]N. G. Petrik and G. A. Kimmel, Phys. Rev. Lett. **90**(16), 166102 (2003).
[16]G. Perluzzo, L. Sanche, C. Gaubert, and R. Baudoing, Phys. Rev. B **30**(8), 4292–4296 (1984).
[17]J. P. Cowin, A. A. Tsekouras, M. J. Iedema, K. Wu, and G. B. Ellison, Nature (London) **398**(6726), 405–407 (1999).
[18]D. L. Scovell, T. D. Pinkerton, V. K. Medvedev, and E. M. Stuve, Surf. Sci. **457**(3), 365–376 (2000).
[19]M. C. Akin, N. G. Petrik, and G. A. Kimmel, J. Chem. Phys. **130**(10), 104710 (2009).
[20]V. F. Petrenko, Electrical Properties of Ice, Special Report 93-20; U.S. Army Cold Regions Research and Engineering Laboratory (CRREL), 1994.
[21]T. Livneh and M. Asscher, J. Phys. Chem. B **104**(14), 3355–3363 (2000).
[22]A. A. Tsekouras, M. J. Iedema, and J. P. Cowin, Phys. Rev. Lett. **80**(26), 5798–5801 (1998).
[23]H. Wang, R. C. Bell, M. J. Iedema, G. K. Schenter, K. Wu, and J. P. Cowin, J. Phys. Chem. B **112**(20), 6379–6389 (2008).
[24]*CRC Handbook of Chemistry and Physics*, 85th ed., edited by D. R. Lide (CRC Press, Boca Raton, FL, 2004–2005).
[25]K. N. Joshipura, J. Phys.: Conf. Ser **80**, 012008 (2007).
[26]S. Bag, M. R. S. McCoustra, and T. Pradeep, J. Phys. Chem. C **115**(28), 13813–13819 (2011).
[27]M. Akbulut, T. E. Madey, and P. Nordlander, J. Chem. Phys. **106**(7), 2801–2810 (1997).
[28]R. N. Barnett, U. Landman, and A. Nitzan, Phys. Rev. Lett. **62**(1), 106–109 (1989).
[29]G. Bader, G. Perluzzo, L. G. Caron, and L. Sanche, Phys. Rev. B **30**(1), 78–84 (1984).
[30]F. Baletto, C. Cavazzoni, and S. Scandolo, Phys. Rev. Lett. **95**(17), 176801 (2005).
[31]H. Dosch, A. Lied, and J. H. Bilgram, Surf. Sci. **327**(1-2), 145–164 (1995).
[32]W. C. Simpson, M. T. Sieger, T. M. Orlando, L. Parenteau, K. Nagesha, and L. Sanche, J. Chem. Phys. **107**(20), 8668–8677 (1997).
[33]W. C. Simpson, T. M. Orlando, L. Parenteau, K. Nagesha, and L. Sanche, J. Chem. Phys. **108**(12), 5027–5034 (1998).
[34]M. Fisher and J. P. Devlin, J. Phys. Chem. **99**(29), 11584–11590 (1995).
[35]M. T. Sieger, W. C. Simpson, and T. M. Orlando, Phys. Rev. B **56**(8), 4925–4937 (1997).
[36]T. M. Orlando and G. A. Kimmel, Surf. Sci. **390**(1–3), 79–85 (1997).
[37]V. F. Petrenko and R. W. Whitworth, US Army Corps of Engineers, Special Report 94-4, 1994.
[38]S. Pnevmatikos, Phys. Rev. Lett. **60**(15), 1534–1537 (1988).
[39]I. Takei and N. Maeno, J. Phys. **48**(C-1), 121–126 (1987).
[40]L. Delzeit, M. S. Devlin, B. Rowland, J. P. Devlin, and V. Buch, J. Phys. Chem. **100**(24), 10076–10082 (1996).
[41]J. P. Devlin and V. Buch, J. Phys. Chem. **99**(45), 16534–16548 (1995).
[42]B. Rowland, N. S. Kadagathur, J. P. Devlin, V. Buch, T. Feldman, and M. J. Wojcik, J. Chem. Phys. **102**(21), 8328–8341 (1995).
[43]J. Zhao, B. Li, K. Onda, M. Feng, and H. Petek, Chem. Rev. **106**(10), 4402–4427 (2006).
[44]K. D. Jordan and M. A. Johnson, Science **329**(5987), 42–43 (2010).
[45]M. P. Seah and W. A. Dench, Surf. Interface Anal. **1**(1), 2–11 (1979).

[46]M. Bertin, M. Mever, J. Staehler, C. Gahl, M. Wolf, and U. Bovensiepen, Faraday Discuss. **141**, 293–307 (2009).
[47]K. Kobayashi, J. Phys. Chem. **87**(21), 4317–4321 (1983).
[48]T. Hama, M. Yokoyama, A. Yabushita, M. Kawasaki, S. Andersson, C. M. Western, M. N. R. Ashfold, R. N. Dixon, and N. Watanabe, J. Chem. Phys. **132**(16), 164508 (2010).
[49]M. Wolf, S. Nettesheim, J. M. White, E. Hasselbrink, and G. Ertl, J. Chem. Phys. **94**(6), 4609–4619 (1991).
[50]K. I. Oberg, H. Linnartz, R. Visser, and E. F. van Dishoeck, Astrophys. J. **693**(2), 1209–1218 (2009).
[51]J. R. R. Verlet, A. E. Bragg, A. Kammrath, O. Cheshnovsky, and D. M. Neumark, Science **307**(5706), 93–96 (2005).